J Mol Model (2004) 10:393–398
DOI 10.1007/s00894-004-0212-y

ORIGINAL PAPER

Pranab K. Mohapatra · Adikanda Khamari · Mukesh K. Raval

A method for structural analysis of α-helices of membrane proteins

Received: 21 May 2004 / Accepted: 1 September 2004 / Published online: 4 November 2004

Abstract A method has been developed to calculate and represent the geometry of α-helices of membrane proteins. Geometrical parameters are computed from coordinate files in the protein data bank. The axis of the helix is determined from the local centroids of tetrapeptide units of the helix. The method provides lower and upper cutoff values of the distance between backbone atoms C_i(carbonyl carbon) and N_{i+4} for allocation of a hinge in a helix. The method calculates other geometrical parameters like the length of helix, twist per residue, height per residue, kink and swivel angles. Packing of bundles of α-helices is represented by relative angles of inclination and distance vectors. The parameters are useful in quantitative descriptions of structural features of membrane proteins.

Keywords Transmembrane helix · Helix parameters · Hinge · Kink · Swivel

Introduction

Transmembrane α-helix bundles are a major regular structural feature of membrane proteins barring porins, where the presence of β-strands is observed. The structural parameters of helices may be useful in understanding the organization and function of the proteins. A database of helical parameters from various proteins may be useful in assigning structural patterns and evolving design principles.

Determination of the axis of a helix is the primary step in computing other helical parameters. Several methods have been employed to determine the axis; the linear least squares fit method being the most suitable for irregular helices [1]. In this method a straight line is determined such that sum of the square of the distances of Cα atoms from the line is minimum. Another approach fits the consecutive frames of backbone atoms of a helix to five residues of an ideal helix and the projections of backbone atoms on the axis of the ideal helix give points from which the central axis of the helix is constructed [2]. Further, in some cases helices may be kinked or curved. One of the causes of a perturbation in linearity of axis is the presence of Pro in the middle of the helix [2–4]. The perturbation induces a hinge in the helix. Identification of a hinge residue is made by various methods. Perturbation in backbone dihedral angles (Φ, Ψ) may indicate a hinge [2]. An outlying virtual dihedral angle formed by four consecutive Cα atoms in a backbone (Cα_i, Cα_{i+1}, Cα_{i+2}, Cα_{i+3}) may be an indicator of a hinge [4]. Except for hinges induced by Pro, these methods do not provide a sharp cutoff value for inference of a hinge. The hinge residue is defined as the residue that allows the best least squares fit of two lines to the estimated helix axis of the segments before and after the hinge [2]. Kumar and Bansal [5, 6] suggest yet another method. They computed local helix parameters for every four consecutive Cα atoms. This window of four Cα atoms is slid through the entire helix. If the maximum local helix bending angle is $\geq$20°, the helix is classified as kinked, otherwise it is subjected to a test for curvature or linearity. If the root mean square deviations both for the line (rmsL) and the circle (rmsC) fitted to the local origins of the helix are <1 Å, the ratio rmsL/rmsC is determined. If the ratio is >1 the helix is termed curved and if it is $\leq$0.7 the helix is classified as linear [5, 6]. Both linear and curved helices are indicated if the ratio is between 0.7 and 1.0. In that case, the square of linear correlation coefficient (r^2) decides the helix class. If $r^2 \geq$ 0.8 the helix is linear. If $r^2 \leq 0.5$ the helix is curved. However, if $0.8 > r^2 > 0.5$ the helix type is ambiguous. The method, however, does not consider swivel in the helix. All these methods apply algorithms for three-dimensional best fit. Again, these methods leave scope for searching for a better method to identify hinge residues unambiguously.

P. K. Mohapatra · M. K. Raval (✉)
Post Graduate Department of Chemistry,
Government College,
Sundargarh, 770002, Orissa, India
e-mail: mkroval@sancharnet.in

A. Khamari
Department of Physics,
Rajendra College,
Bolangir, 767002, Orissa, India

In the present work, we use a simple algorithm to estimate the helix axis, which does not require any rigorous statistics. Local centroids are computed using coordinates of Cα atoms of consecutive tetrapeptide units of a helix and finally the axis is constructed from the local centroids. The method suggests a new parameter for identification of hinge residues. The hinge residue is located with a change in distance beyond a cutoff value between the C_i (carbonyl carbon of backbone) and N_{i+4} atoms. The method also uses molecular visualization software to assist the theoretical computations. Structural parameters describe the organization of helix bundles in membrane proteins.

Methodology

Coordinate files of X-ray structures of membrane proteins were selected from the protein data bank for determining the helical parameters.

Determination of α-helical regions

Dihedral angles were computed from the coordinate files using an in-house program MAPMAK [7] and listed for each residue along with an assignment of the conformational status of the residue (right or left helical, β-strand, or unknown if it does not fall into the category of regular structures). A clustering of helical conformation for more than 15 consecutive hydrophobic residues was taken to indicate transmembrane helical regions. The molecular visualization tools RASMOL [8] and MODELYN [9] were used to confirm the transmembrane α-helical regions and helices lying in the inner or outer side of the membrane visually. MODELYN was also used for building an ideal α-helix model of poly-$(Ala)_{15}$ with Φ, Ψ, ω values of -57, -47 and 180° [10].

Computation of helix axis

Approximate local centroids Θ'_i (x_i^0, y_i^0, z_i^0) of the helix were determined by taking a frame of a tetrapeptide unit.

$$x_i^0 = \frac{1}{4}\sum_{i}^{i+3} x_i \quad y_i^0 = \frac{1}{4}\sum_{i}^{i+3} y_i \quad z_i^0 = \frac{1}{4}\sum_{i}^{i+3} z_i \tag{1}$$

where x_i,, y_i, and z_i are coordinates of Cα atoms of the tetra peptide frame.

A unit vector in the direction of the resultant of vectors $\Theta'_i\,\Theta'_{i+1}$ yields direction cosines (l, m, n) of the axis of helix (**A**). The axis must pass through the centroid of the helix $\Theta^0=(X^0, Y^0, Z^0)$.

$$\text{i.e.} \quad X^0 = \frac{1}{n}\sum_{i=1}^{n} x_i \quad Y^0 = \frac{1}{n}\sum_{i=1}^{n} y_i \quad Z^0 = \frac{1}{n}\sum_{i=1}^{n} z_i \tag{2}$$

where n is the number of residues in a helix. Refined local centers Θ_i of the helix are then calculated for each C$\alpha$by computing the foot of the perpendicular drawn from Cα_i to **A**. The distance between Cα_i and Θ_i, d(Cα_i Θ_i), gives the radius of the helix, $d(\Theta_i\,\Theta_{i+1})$ gives the height per residue (h) and the dihedral angle formed by Cα_i Θ_i Θ_{i+1}Cα_{i+1} yields the twist per residue (t). If t<0 the helix is left-handed and if t>0 it is right-handed. The distance $d(\Theta_1\,\Theta_n)$ gives the length of the helix. The center Θ^0 (i) of ith helix is defined as

$$\Theta^0(i) = \Theta_{(n+1)/2} \quad \text{if } n \text{ is odd} \tag{3}$$

$$\Theta^0(i) = \frac{1}{2}(\Theta_{n/2} + \Theta_{(n/2)+1}) \quad \text{if } n \text{ is even} \tag{4}$$

Location of hinges

The distance $d(C_iN_{i+4})$ is 4.227±0.014 Å for an ideal α-helix, where C_i is the backbone carbonyl carbon of the ith residue and N_{i+4} is the backbone peptide nitrogen of the i+4th residue and $d(O_iN_{i+4})$ is 3.150±0.107, where O_i is the backbone carbonyl oxygen of the ith residue. As O_i and $(NH)_{i+4}$ form an H-bond, the distance $d(O_iN_{i+4})$ also depends on the strength of the H-bond and vice versa. The parameter $d(C_iN_{i+4})$ is less disperse, includes non-bonded atoms on the helix backbone, and almost parallel to the helix axis. Hence, $d(C_iN_{i+4})$ is chosen for locating perturbations in the helix axis. This parameter deviates in the range of 0.35 Å in straight helices in real cases. Any deviation beyond this may reflect a hinge at the ith residue in the helix. A hinge is quantified by two parameters, kink and swivel [2].

Kink. Depending on the number of hinges in a helix, the axes for parts of the helix are determined from the beginning to the first hinge residue to give the $\mathbf{A}_1$ axis. From the hinge to the next hinge (or end) gives the $\mathbf{A}_2$ axis and so on. The angle between $\mathbf{A}_1$ and $\mathbf{A}_2$ yields the value of the kink.

Swivel. The angle between **N1**,normal to $\mathbf{C}\alpha_h$ Θ_h and $\mathbf{A}_1$, and **N2**, normal to $\mathbf{A}_1$ and $\mathbf{A}_2$, gives the swivel angle, where the subscript h designates Cα and O_i (the local helix center) of the hinged residue.

Organization of helices

The distance vector ($\mathbf{d}_{ij}$) between centers and the relative orientation Ω_{ij} of the axes of the helices i to j results in a display of the relative organization of helices in membrane proteins. Ω_{ij} is defined as the dihedral angle formed by $[\Theta_n(i)\Theta^0(i)\Theta^0(j)\Theta_n(j)]$. Arrangement of the parameters in a tabular format or visualization by graphics represents the structure of a helix bundle in a protein.

Location of neighboring atoms

The atoms located in a given neighborhood of an atom are determined from a coordinate file in PDB format by an in-house program METAL [11] and PDBENV [12]. This program was used to detect the amino-acid residues that form ligands for metal ions or H-bonds to neighboring moieties.

Results

Structural analysis of ideal α-helix

An ideal α-helix (H0) with 15 Ala residues was constructed using the modeling software MODELYN. The bond lengths, bond angles and dihedral angles are shown in Table 1. A structural analysis yields ideal $d(C_iN_{i+4})$ values of 4.227±0.014 Å . The values for radius (r), height per residue (h), and twist per residue (t) are 2.280± 0.020 Å, 1.55±0.021 Å, and 99.1±0.8°, as determined by the present method. Analysis of ideal helix provides the ideal value for $d(C_iN_{i+4})$ and proves the validity of the method for determining helix parameters.

Comparison of results obtained by present method with least square method

The axes of 15 different α-helices were determined by the method described above as well as by the least squares

Table 1 Parameters of monomers of the model helix

Bondlengths (Å)	
Cα–C	1.532
Cα–Cβ	1.529
Cα–N	1.469
C=O	1.238
C–N	1.320
Bond angles (°)	
N–Cα–C	111.0
N–Cα–Cβ	110.1
N–C–O	120.0
C–Cα–Cβ	110.3
Cα–C–N	115.7
C–N–Cα	120.3
Cα–C–O	120.1
Dihedral angles (°)	
Φ	–57.0
Ψ	–47.0
ω	180.0

method [1]. Table 2 gives the results. The axes determined by our method deviate from those by the least squares method in the range of 0–2.7°. The root mean square deviation is 1.789°. This reflects that the accuracy of the present method is comparable to that of the standard least squares method for determining helix axes.

Identification of hinge residue in transmembrane helices

Hinge residues in some transmembrane α-helices of different membrane proteins were identified by analyzing the $d(C_iN_{i+4})$ parameter. Kink and swivel angles at the hinges are given in Table 3.

Structural analysis of light harvesting protein LHC II type I

The method was used to analyze the structural parameters of transmembrane helices of light harvesting protein of photosystem II (LHC II, Type I) (PDB ID1RWT [13]) as

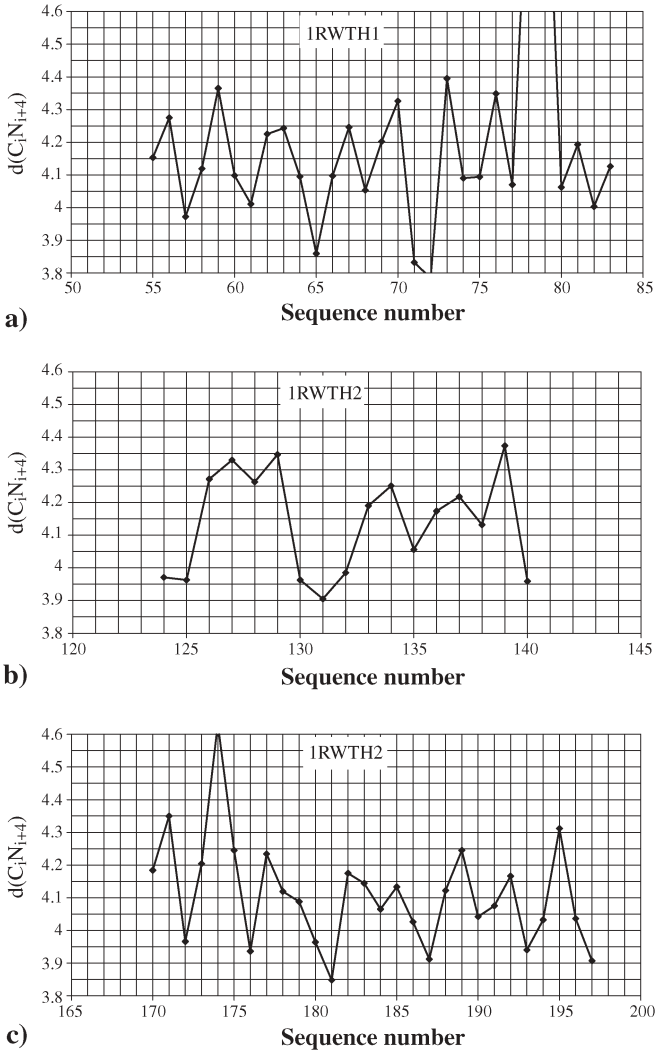

Fig. 1 Plots depicting distances between C_i and N_{i+4} at residues of the helices H1 (**a**), H2 (**b**), and H3 (**c**) of the light harvesting protein LHC II Type I (PDB ID 1RWT [13]).

Table 2 Comparison of helix axes determined by the least squares and centroid methods

Sl. No.	PDB ID	Name of protein	Helix sequence	Deviation in degree
1	–	Model ideal helix Ala_{15}	1–15	2.598
2	1PRC (L-subunit)	Photosynthetic reaction center *R. viridis*	84–111	0
3	1PRC (M-subunit)	Photosynthetic reaction center *R. viridis*	53–76	0
4			111–138	1.900
5	1RWT	Light harvesting complex II—type I *S. oleracea*	124–144	2.301
6	1DIY	Prostaglandin H2 synthase-1 *O. aries*	296–318	2.733
7			325–347	2.289
8	1AQ1	Cyclin dependent protein kinase-2 *H. sapiens*	101–121	0
9			182–198	0.499
10	1JB0 (A-subunit)	Photosystem I *S. elongatus*	65–96	2.509
11			155–182	0
12	1JB0 (B-subunit)	Photosystem I *S. elongatus*	38–69	2.731
13			131–156	1.065
14	1AFO	Glycophorin A *H. sapiens*	72–99	0.738
15	1J4N	Aquaporin 1 *B. taurus*	139–159	1.996

The angle in degrees between the axes determined by the two methods is expressed as a deviation

Table 3 Detection of hinges in some transmembrane helices

Sl. No.	PDB ID	Name of protein	Helix sequence	Hinge position(s)	Hinge	
					θ^a	τ^a
1	1PRC (L-subunit)	Photosynthetic reaction center *R. viridis*	115–164	Leu119	23.1	54.9
				Cys129	30.2	1.9
				Leu131	3.8	−64.1
2			171–198	Leu189	4.2	−61.6
3			226–250	Ala237	36.4	1.6
				Leu242	28.5	−7.5
4	1PRC (M-subunit)	Photosynthetic reaction center *R. viridis*	142–166	Ile158	41.9	−39.0
5			198–227	Gly205	9.5	17.6
6			260–284	Ser271	24.0	−60.2
7	1JB0 (A-subunit)	Photosystem I *S. elongatus*	193–218	His199	9.3	65.7
8	1JB0 (B-subunit)	Photosystem I *S. elongatus*	170–195	His176	11.6	65.2
9	1VF5	Cytochrome b6 *M. laminosus*	33–56	Gln47	10.2	−65.2
10			79–107	Met92	16.3	−69.6
				Val101	3.7	65.7
11			116–139	Val133	14.5	48.0
12			117–205	His187	29.7	−81.7
				Ile195	5.6	0.0
13	1J4N	Aquaporin 1 *B. taurus*	5–36	Arg13	9.2	3.2
				Ser31	35.3	88.8
14			93–117	Val105	5.6	18.5
				Ala112	24.5	−14.6
15			170–189	Phe176	7.9	2.4
				Leu183	46.0	−38.8

[a] Angles θ and τ are in degrees.

Table 4 Helix parameters of the ideal model helix and real helices of the LHC II protein

Helix	Axis	Φ	Ψ	ω	L	r	h	t	Hinge	
									θ	τ
H0	−0.084, −0.995, 0.058	−57.0	−47.0	180.0	23.250	2.280±0.020	1.550±0.021	99.2±0.8	0	0
H1	0.055, 0.609, −0.792	−63.9±6.9	−40.9±8.7	179.8±0.9	48.858	2.273±0.176	1.557±0.365	99.3±14.5	17.5	−28.7
	−0.119, 0.388, −0.914								15.4	29.8
	−0.270, 0.565, −0.780									
H2	−0.194, 0.021, 0.980	−65.8±12.1	−42.0±9.3	180.0±1.0	29.300	2.395±0.423	1.463±0.290	96.2±15.4	0	0
H3	−0.406, −0.638, −0.656	−64.8±9.1	−41.2±6.5	179.8±0.9	45.786	2.340±0.388	1.490±0.350	98.3±13.9	27.6	26.7
	0.019, −0.525, −0.852								5.5	1.5
	0.028, −0.428, −0.904									

Distances are in Å and angles in degrees. n for H0, H1, H2 and H3 are 15, 33, 21 and 32, respectively

an example for this article. LHC II consists of three transmembrane helices H1, H2, and H3.

Location of hinges. The hinges in the helices were detected by plotting $d(C_iN_{i+4})$ against the sequence numbers of the residues, Fig. 1. The analysis shows values of $d(C_iN_{i+4})$ less than 3.877 Å or greater than 4.577 Å i.e., 3.832, 3.784, 5.144, and 5.313 Å at sequences 71, 72, 78 and 79 in H1, suggesting hinges in the helix at Trp71 and Gly78. Similarly, hinges are detected in helix H3 at Ala174 and Ile181, where $d(C_iN_{i+4})$ are 4.633 and 3.848 Å . However, no hinge is suggested in helix H2.

Helix parameters. The parameters of the helices are shown in Table 4. The lengths of helices H1, H2 and H3 are 48.858, 29.300 and 45.786 Å, respectively. The average radii (r) of the helices are in the range 2.272–2.395 Å . The heights per residue (h) are 1.557, 1.463, and 1.490 for H1, H2 and H3, respectively. The range of average values of twist per residue (t) is estimated to be 96.2–99.3°.

Kink and swivel angles. The hinges are quantified in terms of kinks and swivels in degrees (θ, τ). The hinges are (17.5, −28.7) and (15.4, 29.8) in H1 and (27.6, −26.7) and (5.5, −1.5) in H3 (Table 4). The relative orientations (Ω_{ij}) between helices i and j are 154.5° (Ω_{12}), 53.8° (Ω_{13}) and −155.4° (Ω_{23}). Distance vectors $\mathbf{d}_{12}$, $\mathbf{d}_{23}$, $\mathbf{d}_{31}$ are (16.876 **i**, −2.143 **j**, −1.494 **k**), (−24.976 ***i***, 0.853 **j**, 2.307 **k**), and (8.101 **i**, 1.287 **j**, −0.814 **k**), respectively (Table 5). The distances d_{12}, d_{23}, d_{31} are 17.145, 25.005, and 8.302 Å, respectively.

Figure 2 shows helices H1, H2 and H3, while Fig. 3 shows the organization of the helix bundle in terms of the centers of the helices.

Table 5 Parameters of organization of helices

Helix	Center of helix	d_{ij}	d_{ij}	Ω_{ij}
H1	2.715, 21.300, 109.312	16.876 *i*, −2.143 *j*, −1.494 *k*	17.145	154.5
H2	19.591, 19.157, 107.818	−24.976 *i*, 0.856 *j*, 2.307 *k*	25.005	−155.4
H3	−5.335, 24.542, 117.008	8.101 *i*, 1.287 *j*, −0.814 *k*	8.302	53.8

Distances are in Å and angles in degrees

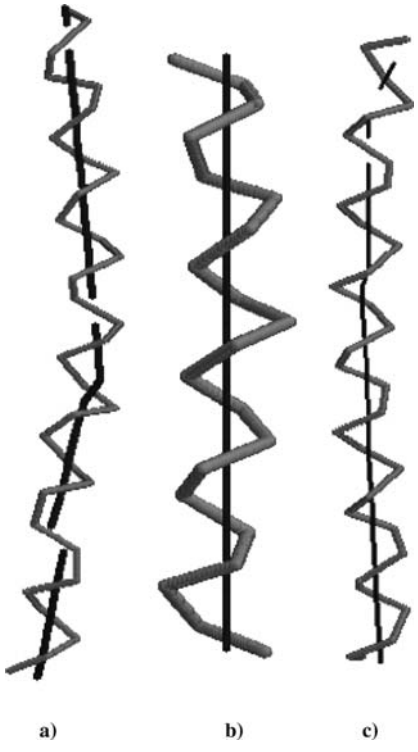

Fig. 2 Backbone representations with axes of helices H1 (**a**), H2 (**b**), and H3 (**c**) of the light harvesting protein LHC II Type I (PDB ID 1RWT [13]). Figures **a**, **b** and **c** were drawn using RASMOL [8].

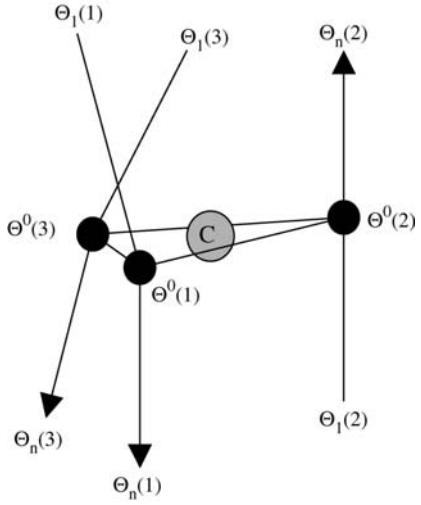

Fig. 3 Representation of the organization of the helix bundle in 1rwt by helix axis $\Theta_1(i)$–$\Theta_n(i)$, helix center $\Theta^0(i)$ of *i*th helix and centroid (*C*) of centers of the three helices. *Arrow-heads* indicate the C-terminal end of a helix.

Discussion

Structural parameters of LHC II

The helix parameters deviate from the ideal value in real cases, as shown by comparison of the values of the ideal helix with helices of LHC II in Table 4. The helix parameters show that the structures of the α-helices of LHC II are close to ones described by Barlow and Thornton [14] and Perutz [15]. The three helices are organized such that their centers lie at the vertices of an irregular triangle (Fig. 3). Helices H1 and H3 are inclined to each other in a crossed pattern. They are closer to each other than to H2. Helices H1 and H3 contain hinges while H2 is straight.

Hinges in α-helices

Hinges in transmembrane helices occur with high frequency [16]. The presence of Pro in the middle of a helix induces a hinge [2–4, 17]. Pro-induced hinges usually occur at the *i*–4th residue. The hinge may be induced by the absence of an H-bond between O of *i*–4th residue and N of Pro because the nitrogen is not available for H-bonding. In addition, because of steric hindrance, H-bonding between O of the *i*–3rd and *i*+1st residues is not possible. For example, hinge Leu119 in the L-subunit of 1PRC is at the *i*+1st position of Pro118 (Table 3). However, hinges may also occur without the presence of a Pro residue. The causative factors for induction of hinges and explanation of their consequences remain to be determined by studying a large number of hinges and correlating the results with organization and functions of proteins.

Significance of Hinges

A hinge is structurally and physiologically a significant feature. Hinges facilitate helix packing in membrane proteins [18]. Many important functions like activation of ion-channel gates [19, 20], receptor activity [21] and functionally essential salt-bridge formation [22] require kinks in helices.

Some examples may highlight the significance of hinges (Table 3). ND1 and NE2 of His190, a neighbor of the hinge residue Leu189 in the L-subunit (1PRC), bonds with O4 of quinoneB (614) (2.669 Å) and Fe (1.990 Å) of the photosynthetic reaction center. Hinges at Ala237 and Leu242 in the L-subunit of 1PRC may facilitate binding of NE2 of His230 with Fe (2.407 Å) and OG1 of Thr248

with OBD (2.627 Å) of bacterial chlorophyll (BChl), designated D_L. Similarly, the hinge at Gly205 in the M-subunit of 1PRC may be required for binding of His200 to Mg (1.890 Å) of BChl, designated D_M, ND1 of His217 to quinoneA (3.108 Å), NE2 of His217 to Fe (2.102 Å). NE2 of the hinge residues His199 (A-subunit, 1JB0) and His176 (B-subunit, 1JB0) form ligands to Mg of antenna Chl110 (2.356 Å) and Chl209 (2.322 Å), respectively. ND1 of these residues form H-bonds with backbone carbonyls of Ser at the *i*–4th position. Hinges at Phe176 and Leu183 probably properly orient His182, which is critical for narrowing the pore in aquaporin (1J4N). Met92 and Val101, His187, and Ile195 bend to favor ligation of His85, His100, His187, and His202 to Fe ions of high and low potential hemes in Cytb6 (1VF5). Hinges at Trp71, Ala174 and Ile181 in 1RWT may facilitate packing of helices along with binding of Chl with the protein matrix. NH1 of Arg70 (1RWT) is at a distance of 2.717 Å from OBD of Chl *b* 608 and NH2 at 2.982 Å, suggesting H-bonding between these atoms. NE2 of His68 (1RWT) is a ligand to Mg of Chl *a* 603 (2.279 Å). OE1 of Glu180 (180) is a ligand to Mg of Chl *a* 610. NZ of Lys182 (1RWT) may form an H-bond with O5 of phosphate group of LHG630 (2.694 Å). O4 of LHG630 serves as a ligand to Mg of Chl *a* 611 (2.357 Å) in 1RWT. However, such an explanation for the hinge at Ala174 (1RWT) is not available.

The method described above uses a simple algorithm compared to existing methods [1, 2] for determining helix axes without compromising accuracy. The method also suggests a distance parameter $d(C_iN_{i+4})$, which can be included in a program for automated detection of hinges in a helix. The method yields a quantitative description of the structure of transmembrane helix bundles (Fig. 3), which may be useful in clustering structural classes of membrane proteins. Such a study may be useful in the structural classification and evolution of a design principle for membrane proteins.

Acknowledgements Permission to use the programs developed by Prof. C. Ramakrishnan, IISc, Bangalore, and a preview version of MODELYN by Dr. C. N. Mandal, IICB, Kolkata, India is gratefully acknowledged.

References

1. Chou KC, Nemethy G, Scheraga HA (1984) J Am Chem Soc 106:3161–3170
2. Cordes FS, Bright JN, Sansom MSP (2002) J Mol Biol 323:951–960
3. Ramachandran GN, Ramkrishnan C, Sasisekheran V (1963) J Mol Biol 7:95–99
4. Sankararamakrishnan R, Vishveshwara S (1990) Biopolymers 30:287–298
5. Bansal M, Kumar S, Velavan R (2000) J Biomol Struct Dyn 17:811–819
6. Kumar S, Bansal M (1998) Biophys J 75:1935–1944
7. Ramakrishnan C, MAPMAK. Indian Institute of Science, Bangalore
8. Sayle RA, Milner-White EJ (1995) Trends Biochem Sci 20:374–376
9. Mandal CN, MODELYN. Indian Institute of Chemical Biology, Kolkata
10. Arnott S, Wonacott AJ (1966) J Mol Biol 21:371–383
11. Ramakrishnan C (1996) METAL. Indian Institute of Science, Bangalore
12. Raval MK (1996) PDBENV. Rajendra College, Balangir
13. Liu Z, Yan H, Wang K, Kuang T, Zhang J, Gui L, An X, Chang W (2004) Nature 428:287–292
14. Barlow DJ, Thornton JM (1988) J Mol Biol 201:601–619
15. Perutz MF (1951) Nature 167:1053–1058
16. Yohannan S, Faham S, Yang D, Whitelegge JP, Bowie JU (2004) Proc Natl Acad Sci U S A 101:959–963
17. von Heijne G (1991) J Mol Biol 218:499–503
18. Ceruso MA, Weinstein H (2002) J Mol Biol 318:1237–1249
19. Bright JN, Shrivastava IH, Cordes FS, Sansom MS (2002) Biopolymers 64:303–313
20. Harrris T, Graber AR, Covarrubias M (2003) Am J Physiol Cell Physiol 285:C788–C796
21. Singh R, Hurst DP, Barnett-Norris J, Lynch DL, Reggio PH, Guarnieri F (2002) J Pept Res 60:357–370
22. Vonck J, von Nidda TK, Meier T, Matthey U, Mills DJ, Kuhlbrandt W, Dimroth P (2002) J Mol Biol 321:307–316